Int. J. Hum. Capital Urban Manage., 11(1): 33-50, Winter 2026

International Journal of Human Capital in Urban Management
(IJHCUM)

Homepage: http://www.ijhcum.net/

ORIGINAL RESEARCH PAPER

Modeling sediment transport and assessing erosion and sedimentation status in the Haraz River watershed based on the ecosystem services concept

A. Chahkandi, G. R. Nabi Bidhendi*, B. Malekmohammadi

Department of Environmental Engineering, Faculty of Environment, University of Tehran, Tehran, Iran

ARTICLE INFO

Article History:
Received 31 January 2025
Revised 22 April 2025
Accepted 26 May 2025

Keywords:
Sediment transport
Soil erosion
Ecosystem services
Haraz River watershed
InVEST DSR

ABSTRACT

BACKGROUND AND OBJECTIVES: Effective river basin management requires understanding sediment transport dynamics and their impact on ecosystem services to mitigate soil erosion and sedimentation. This study emphasizes the novel integration of the ecosystem services framework into sediment transport modeling using the Integrated Valuation Ecosystem Services and Tradeoffs Sediment Delivery Ratio model. The Haraz River basin, a critical watershed in northern Iran, faces significant erosion and sedimentation problems due to steep slopes, sporadic vegetation, and intensive land use. This study aimed to model sediment transport and assess erosion and sedimentation dynamics within the basin using the Integrated Valuation of Ecosystem Services and Tradeoffs Sediment Delivery Rate model, focusing on ecosystem services, particularly sediment retention and delivery.

METHODS: The Integrated Valuation of Ecosystem Services and Tradeoffs Sediment Delivery Rate model was applied to the Haraz River Basin, using high-resolution land use maps, a Digital Elevation Model, and field-calibrated parameters. The study quantified soil erosion and sediment export at pixel and sub-watershed levels. The analysis considered key factors such as rainfall erosivity, soil erodibility, slope length, land cover, and management actions to estimate sediment dynamics and identify critical erosion hotspots.

FINDINGS: The results showed considerable spatial variability in sediment transport and retention across the catchment. Subwatershed 2 had the highest soil erosion potential (13,016,268 tonnes) and sediment export (1,992,277 tonnes), primarily due to steep slopes and limited vegetation cover. In contrast, sub-catchment 5 had the lowest erosion potential (60,721 tonnes) and sediment export (9,328 tonnes) due to effective land management and favorable land cover conditions. The values for erosion control and sediment retention illustrate the crucial role of vegetation in mitigating soil loss and reducing sediment input into rivers.

CONCLUSION: This study highlights the complex interplay between natural and management factors in regulating erosion and sediment dynamics. Integrating Sediment Delivery Ratio modeling with an ecosystem services framework provided actionable insights for prioritizing erosion control measures in high-risk areas and improving sediment retention. Management strategies that include vegetation restoration, land use optimization, and sediment control barriers are recommended to improve watershed sustainability in the Haraz Basin.

DOI: 10.22034/IJHCUM.2026.01.03

NUMBER OF REFERENCES	NUMBER OF FIGURES	NUMBER OF TABLES
39	10	2

*Corresponding Author:
Email: *ghhendi@ut.ac.ir*
Phone: +982161113167
ORCID: 0000-0001-9930-9080

Note: Discussion period for this manuscript open until April 1, 2026 on IJHCUM website at the "Show Article.

INTRODUCTION

The sustainable management of river watersheds is critically important for maintaining both ecological integrity and providing vital ecosystem services (Andualem *et al.*, 2023), (Balist *et al.*, 2022a), (Rodriguez *et al.*, 2023). Sediment transport, a fundamental process within river systems, has a substantial impact on several ecosystem services, including water quality, aquatic habitat, and flood protection (Fang *et al.*, 2024; Slosson *et al.*, 2021; Malekmohammadi *et al.*, 2023). However, anthropogenic activities and climate change are altering sediment dynamics and leading to increased erosion and sedimentation in many river basins worldwide (Owens *et al.*, 2020), (Zebardast *et al.*, 2023), (Sadeghi *et al.*, 2021); this requires a comprehensive understanding of the interplay between sediment transport, erosion, sedimentation, and the resulting impacts on ecosystem services. The Sediment Delivery Ratio (SDR) is a significant indicator for managing water catchment areas. It indicates the proportion of sediment generated from land surfaces that is ultimately transported to a particular river or river system point. Understanding sediment dynamics, erosion processes, and their impact on ecosystem services and water resources is fundamental. Increasingly, researchers and practitioners are adopting ecosystem services frameworks to analyze and model sediment dynamics due to their holistic approach, which integrates environmental, social, and economic dimensions (Schröter *et al.*, 2014; Costanza *et al.*, 2017). This study aims to model SDR in a watershed using the Integrated Valuation of Ecosystem Services and Tradeoffs model (InVEST), which explicitly incorporates ecosystem services to assess sediment transport and deposition processes. Sediment delivery processes are closely tied to land-use practices, soil conservation, and hydrological dynamics within a watershed. High sediment loads can lead to several adverse consequences, such as reservoir siltation, reduced water quality, habitat degradation, and increased treatment costs for drinking water (Pimentel *et al.*, 1995). Understanding SDR provides insights into erosion hotspots and helps prioritize areas for conservation interventions (Borrelli *et al.*, 2017). Moreover, sediment transport affects ecosystems' provisioning, regulating, and supporting services, underscoring the need to study SDR from an ecosystem services perspective (Dominati *et al.*, 2010). The ecosystem services concept provides a structured approach to evaluate the benefits humans derive from ecosystems, such as clean water, fertile soils, and flood regulation (MEA, 2005). Sediment dynamics directly influence multiple ecosystem services. For instance, regulating services, including soil retention and water purification, are impacted by sediment transport and deposition patterns. Similarly, cultural services, such as recreational fishing and aesthetic values of water bodies, may be degraded by excessive sedimentation (Posthumus *et al.*, 2010). Integrating SDR modeling within the ecosystem services framework enables a comprehensive understanding of how land-use changes, climate variability, and conservation efforts affect these services. Sediment Transport Modeling: Empirical sediment rating curves (Tabarestani *et al.*, 2022), (Guo *et al.*, 2002), and physically-based sediment transport models will be used to estimate sediment loads. The selection between these methods will depend on the availability of data on sediment grain size distribution and the characteristics of the river bed. The InVEST model is frequently used for assessing ecosystem services and their tradeoffs. It includes a suite of models that estimate the biophysical and monetary values of ecosystem services, including the SDR model, which predicts sediment retention and delivery based on land use, topography, and climate inputs (Hamel *et al.*, 2015), (Balist *et al.*, 2021). The SDR module of InVEST combines GIS-based spatial analysis with process-based algorithms to evaluate sediment retention and identify priority areas for erosion control (Hamel *et al.*, 2015). The model is particularly useful in watersheds with complex land-use patterns, where it can support decision-making for sustainable land and water resource management. Despite significant progress in SDR modeling, several challenges remain. First, the accuracy of SDR predictions depends on the precision and resolution of input data, like land use maps (Balist *et al.*, 2022b), soil properties, and precipitation patterns (Hamel *et al.*, 2017). Second, existing models often do not fully account for sediment processes' temporal variability and spatial heterogeneity, which can lead to uncertainties in predictions (Tedesco *et al.*, 2020). In addition, more empirical studies are needed to validate model results under different environmental conditions and management scenarios (Fu *et al.*, 2011). This study addresses the above challenges

by applying the InVEST SDR model to a specific watershed to evaluate its effectiveness in capturing sediment dynamics within an ecosystem services framework.

This study aims to

(1) Quantify sediment retention and delivery using the InVEST SDR model,

(2) Analyze spatial patterns of sediment transport,

(3) Assess the impact of sediment dynamics on ecosystem services,

(4) Provide land-use planning recommendations.

This study contributes to the growing literature on sustainable watershed management by integrating SDR modeling with the ecosystem services approach. It provides actionable insights for policymakers, land managers, and conservationists seeking to balance ecological and socio-economic objectives. The paper's structure follows: The methodology section describes the study area, data collection, and modeling approach, including applying the InVEST SDR model. The results section presents the spatial patterns of sediment delivery and retention and their implications for ecosystem services. The significance of the findings is discussed in the context of watershed management and ecosystem services, including limitations and future research directions. The conclusion summarizes the key findings and provides recommendations for sustainable management practices.

MATERIAL AND METHODS

Study region

The study region is located in the southern part of Mazandaran Province, within the political boundaries of Amol County and the Haraz River Basin. The watershed spans 200,051 hectares, with a perimeter of 296.062 kilometers. The basin's minimum elevation is 200 meters, while its maximum elevation reaches 5,600 meters. All rivers within the basin ultimately flow into the Haraz River. Notable rivers include Akhn Sar, Shirkalarud, and Namarestagh. Significant elevations in the basin include Mount Damavand, the highest peak in the region, as well as Shim Kuh and Mount Imamzadeh Qasem. Major settlements within the Haraz watershed include Polour, Nashel, Tiran, Rineh, Kandovan, Ab Esk, Gazanak, Baijan, Balghalm, and others. Fig. 1 illustrates the position of the Haraz study area in Mazandaran Province and the entire country. The Haraz River Basin has a humid to semi-humid climate, with an average annual precipitation of approximately 850 mm, most of which occurs in the fall and winter seasons. Mean annual temperature ranges from 5°C in the highlands to 18°C in lower elevations. The dominant vegetation

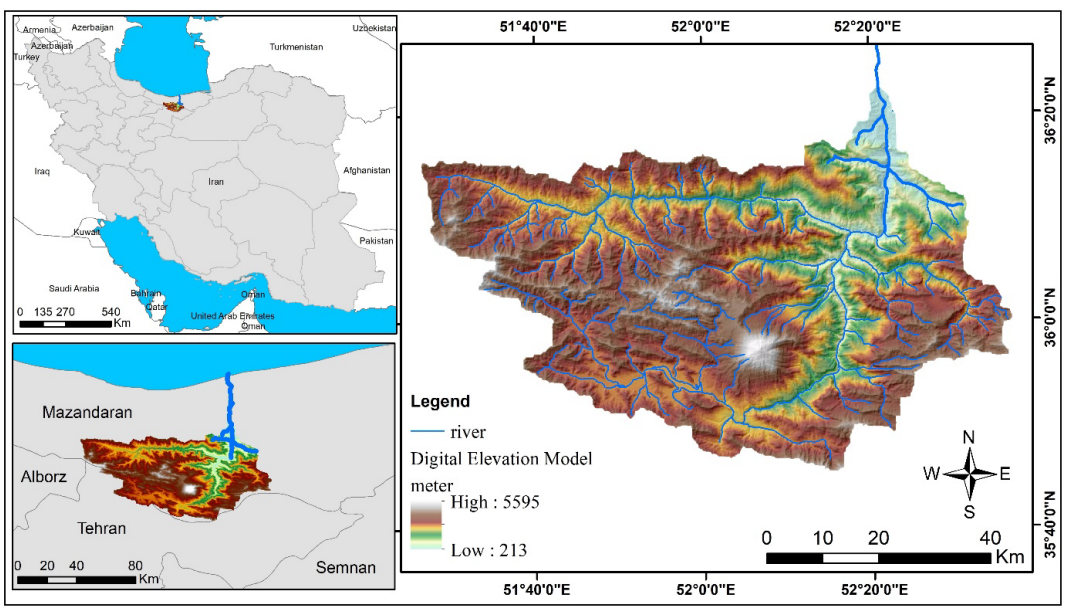

Fig. 1: Location of the study area

types include pasturelands, natural rangelands, and forests, particularly in the northeastern parts of the basin.

Methods

Sediment delivery

The SDR module is a spatially unambiguous model that aligns with the input Digital Elevation Model (DEM) resolution. It estimates the annual soil loss for each pixel and subsequently determines the SDR, quantifying the fraction of eroded soil that reaches the stream. Once sediment enters the stream network, it is assumed to be transported directly to the catchment outlet, as in-stream processes that could modify sediment loads are not considered in this model. Originally introduced by Borselli et al. (2008), this approach has gained increasing recognition in recent studies (e.g., Cavalli *et al*., 2013; López-Vicente *et al*., 2013; Sougnez *et al*., 2011). For more details, refer to the user manual section titled differences between the InVEST SDR model and the original approach by Borselli *et al.,* (2008).

Land use/land cover (LU/LC) data were obtained from ESRI land cover 2024. The DEM was derived from the Shuttle Radar Topography Mission (SRTM) with a 30-meter resolution. Rainfall erosivity data (R-factor) were calculated using long-term monthly rainfall data (1990–2020) obtained from the Iran Meteorological Organization (IRIMO).

Annual soil loss

The annual soil loss for a given pixel (*i*), denoted as *uslei* (expressed in tons per hectare per year), is determined using the Revised Universal Soil Loss Equation (RUSLE). (RUSLE1 - Renard *et al*., 1997):

$$usle_i = Ri \cdot Ki \cdot LSi \cdot Ci \cdot Pi \quad (1)$$

where

- Ri is erosivity of rainfall (units: MJ·mm(hectare per hour per year)−1),
- Ki is the erodibility of soil (units: ton·hectare·hour(MJ·ha·mm)−1),
- LSi is the factor of slope length-gradient (unitless)
- Ci is the factor of cover management (unitless)

Additionally, *Pi* represents the support practice factor, which accounts for the effects of conservation practices in reducing soil erosion (Renard *et al*., 1997; see also Bhattarai and Dutta, 2006). This factor is dimensionless. The *LSi* factor, which accounts for the influence of slope length and steepness on erosion, is derived using the method proposed by Desmet and Govers (1996) for a two-dimensional surface:

$$LS_i = S_i \frac{(A_{\{i-in\}} + D^2)^{m+1} - A_{i-in}^{m+1}}{D^{m+2} \cdot x_i^m \cdot (22.13)^m} \quad (2)$$

where

- The parameter *Si* represents the slope factor of grid cell *i*, computed as a slope gradient function. In this context, *s* denotes the percentage slope, while ϑ represents the slope angle in degrees (Renard *et al*., 1997).

$$S = \begin{cases} 10.8 \cdot \sin(\theta) + 0.03, & where\, s < 9\% \\ 16.8 \cdot \sin(\theta) - 0.50, & where\, s \geq 9\% \end{cases}$$

The parameter Ai−in represents the contributing area (m²) at the inlet of a grid cell, which is derived using the Multiple-Flow Direction (MFD) method. This approach distributes flow across multiple downslope directions, providing a more accurate representation of surface runoff and soil erosion processes.

- D is the linear dimension of the grid cell (m)
- *xi* represents the aspect mean, weighted by the proportional outflow from grid cell *i*, as determined using the MFD algorithm. It is calculated by

$xi = |\sin \alpha_i| + |\cos \alpha_i|$

- where α_i Represents the radian angle for direction d, and P denotes the proportion of total outflow from cell i in direction d.
- -m is the length exponent factor in the RUSLE.

The maximum slope length is limited to 122 meters to prevent overestimating the LS factor in heterogeneous landscapes, though this Threshold can be adjusted as a user-defined parameter (Desmet and Govers, 1996; Renard *et al*., 1997). The length exponent *m* in the LS factor is derived from the traditional Universal Soil Loss Equation (USLE), as explained by Oliveira *et al*. 2013).

$$m = \begin{cases} 0.2 & where\ \theta \le 1\% \\ 0.3 & where\ 1\% < \theta \le 3.5\% \\ 0.4 & where\ 3.5\% < \theta \le 5\% \\ 0.5 & where\ 5\% < \theta \le 9\% \\ \beta/(1+\beta) & where\ \theta > 9\% \end{cases}$$

$$\beta = \frac{sin\theta / 0.0896}{3sin\theta^{0.8} + 0.56}$$

SDR

Step 1: Calculation of the Connectivity Index (IC)

Following the methodology proposed by Borselli *et al.* (2008), the model first calculates the IC for each pixel. This index quantifies the hydrological connection between sediment sources (i.e., eroded material from the landscape) and sediment sinks (such as streams). A higher IC value indicates a stronger connection, meaning that a greater proportion of sediment from an upstream pixel is transported to a downslope sink, for example, a stream. Strong connectivity is typically observed when the flow path between sediment sources and sinks is steep, short, or sparsely vegetated. Conversely, lower IC values correspond to areas with dense vegetation and gentler slopes, where sediment transport is less efficient. The *IC* is determined by two key factors:

1- The upslope contributing area (Dup)

2- The flow path distance to the nearest stream (Ddn).

Suppose the upslope area is extensive but has a gentle slope and dense vegetation (reflected in a low USLE C factor). In that case, *Dup* will be lower, indicating a reduced likelihood of sediment reaching the stream. Similarly, if the downslope flow path to the stream is long, characterized by low slopes and substantial vegetative cover, *Ddn* will also be low, further limiting sediment transport. IC is calculated as follows:

$$IC = log_{10}\left(\frac{Dup}{Ddn}\right) \quad (3)$$

Threshold values for slope (Sth) and cover-management factor (Cth) are applied in the computation of Dup and Ddn. To prevent infinite values in the IC, a lower bound is established.

An upper bound is imposed on the slope to minimize distortions caused by excessively high IC values in steep areas. These constraints help control extreme values and ensure more accurate sediment connectivity calculations (Cavalli *et al.*, 2013).

$$Sth = \begin{cases} 0.005 & for\ S < 0.005 \\ S & for\ 0.005 \le S \le 1 \\ 1 & for\ S > 1 \end{cases} \quad (4)$$

$$Cth = \begin{cases} 0.001 & for\ C < 0.001 \\ C & otherwise \end{cases} \quad (5)$$

Dup is the upslope component defined as:

$$\mathrm{Dup} = \bar{C}_{th}\bar{S}_{th}\sqrt{\mathrm{A}} \quad (6)$$

$\bar{C}_{th}$ represents the average thresholded C factor for the upslope contributing zone, while $\bar{S}_{th}$ denotes the average thresholded slope gradient of the upslope study area (expressed in m/m). *A* corresponds to the upslope contributing area (measured in m²), delineated using the Multiple-Flow Direction (MFD) algorithm. The downslope factor (*Ddn*) is determined as follows:

$$D_{dn} = \sum_i \frac{d_i}{C_{th,i}S_{thi}} \quad (7)$$

Here, d_i represents the length of the flow path across the *i*-th cell, determined based on the steepest downslope direction (measured in meters). The parameters *Cth,i* and *Sth,i* correspond to the thresholded cover-management factor and slope gradient for the *i*-th cell. Like the upslope component, the downslope flow path is derived using the MFD algorithm.

Step 2: Calculation of the SDR

The SDR for a specified pixel *i* is determined based on the IC using the following approach (Vigiak *et al.*, 2012):

$$SDR_i = \frac{SDRmax}{1 + \exp\left(\frac{IC_0 - IC_i}{k}\right)} \quad (8)$$

SDRmax represents the maximum theoretical SDR, which is adjusted to an average value of 0.8, as

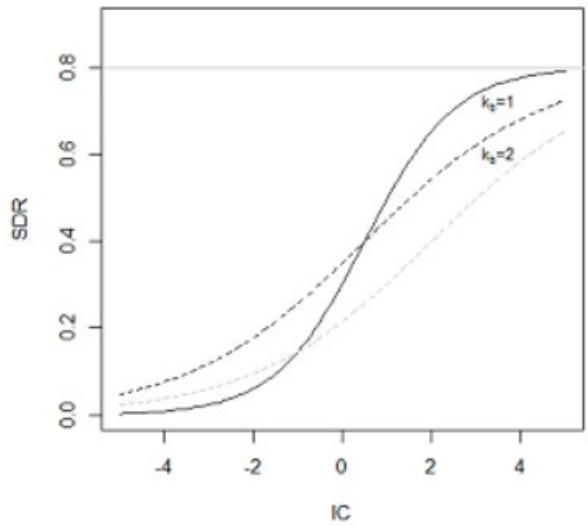

Fig. 2: Relationship between the SDR and the IC (Hamel et al., 2015)

suggested by (Vigiak *et al*., 2012). The parameters IC0 and k serve as calibration factors that shape the relationship between SDR and the IC, which follows an increasing function. The influence of IC0 and k on SDR is demonstrated in the following representation:

The maximum SDR is fixed at SDRmax 0.8. The influence of calibration is demonstrated by setting kb=1 and kb=2 (represented by solid and dashed lines, respectively), while IC0=0.5 and IC0=2 are shown using black and grey dashed lines, respectively.

Sediment export

The sediment export from a given pixel *i*, denoted as *Ei* (measured in tons/hectare /year), represents the portion of eroded sediment from that pixel that ultimately reaches a stream. It is calculated using the following equation:

$$E_i = usle_i \cdot SDR_i \tag{9}$$

The total exported sediment from the catchment, represented as *E* (in tons per hectare per year), is considered as the sum of the sediment transported from all pixels that reach the stream. It is expressed using the following equation:

$$E = \sum_i E_i \tag{10}$$

If relevant data are available, they can be used for calibration or validation with other sediment sources.

Sediment downslope trapping

This model also quantifies the sediment trapped, deposited, or reserved along the downslope flow path from its source. This represents eroded and exported sediment from a pixel but does not ultimately reach the stream. Understanding the spatial distribution of trapped sediment enables users to assess the net sediment change at a pixel level (either a gain or loss), which can be useful for land degradation assessments (Sadeghi *et al*., 2014). Eq. 9 describes sediment export to the stream from pixel *i*. The remaining component in the mass balance equation derived from the USLE accounts for the sediment that does not reach the stream. This loaded sediment must be retained somewhere along the landscape before reaching the stream and is demarcated as follows:

$$E_i^{'} = usle_i \left(1 - SDR_i\right) \tag{11}$$

Since the SDR inherently considers the downslope flow path and biophysical attributes that influence sediment filtration into the stream, the sediment export from a pixel (*Ei*) account for these factors. Consequently, the downslope movement of the remaining sediment flux (*Ei'*) can be modeled independently from *Ei*. To achieve this, the following assumptions about how SDR and sediment export (*Ei*)

behave across a landscape are made:

Property A: SDR increases monotonically along a downhill flow path

As sediment moves downslope, SDR values increase progressively since the distance to the stream decreases. However, in some cases, a downslope pixel may have the same SDR value as an upslope pixel. When this occurs, it indicates that no on-pixel sediment trapping occurs along that step.

Property B: All non-exported sediment flux on a boundary stream pixel is retained at that pixel. If a pixel (*i*) drains directly into a stream, no further downslope filtering of *Ei* occurs. Since *Ei* is the inverse of *Ei'*, this means that the upslope sediment flux (denoted as *Fi*) must have been completely retained on that pixel. Based on these two properties, the amount of *Ei* trapped within a pixel must be a function of:

- The absolute difference in SDR values between pixel i and the downslope pixel(s) it drains into and
- The proximity of the downslope pixel's SDR value to 1.0, indicating how close it is to a stream pixel.

These dynamics can be represented through a linear interpolation of the SDR value difference between pixel *i* and its downslope counterpart relative to the difference between pixel *i*'s SDR and the theoretical highest downslope SDR value of 1.0. Formally, this relationship is expressed as:

$$dTi = \frac{\left(\sum_{k \in \{directly\ downslope\ from\ i\}} SDRk \cdot p(i,k)\right) - SDRi}{1.0 - SDRi} \quad (12)$$

T represents the process of sediment trapping, while *d* in *dTi* denotes a delta difference, indicating the change in sediment trapping. The term *p (i, k)* refers to the proportion of flow from pixel *i* to pixel *k*. This notation is designed to conceptually resemble the derivative of Ti to emphasize the rate of change in sediment trapping.

- In the case of Property A (where downslope $\left(\sum_{\in \{directly\ downslope\ from\ i\}} SDRk \cdot p(i,k)\right) = SDRi$
- When dT=0, it signifies that no portion of F is retained on the pixel.
- In the case of Property B, where the downslope SDR equals 1 (indicating a stream pixel), dT = 1, meaning that the remaining F is retained on the pixel.

Next, we express the amount of sediment flux trapped on each pixel along the flow path by expressing dT as a weighted function of upslope flux.

$$Ti = dTi \cdot \left(\sum_{j \in \{pixels\ that\ drain\ to\ i\}} Fj \cdot p(i,j) \right) \quad (13)$$

Here, *Fi* represents the sediment export flux from pixel *i* that fails to reach the stream. This flux is quantified as follows:

$$Fi = (1 - dTi) \cdot \left(\left(\sum_{j \in \{pixels\ that\ drain\ to\ i\}} Fj \cdot p(i,j) \right) + Ei' \right) \quad (14)$$

Ecosystem service indicators

The landscape's potential ecosystem service of erosion control is evaluated through two approaches:

Avoided erosion – These measures how vegetation helps prevent soil erosion at the pixel level. In other words, it evaluates the value of vegetation in minimizing erosion from occurring in the first place. This metric is useful for quantifying the ecosystem service in terms of local soil loss prevention and is calculated as:

$$AERi = RKLSi - USLEi \quad (15)$$

AERi represents the avoided erosion on pixel i, calculated as the difference between RKLSi and USLEi. This difference reflects the benefit of vegetation and effective land management practices, as RKLS corresponds to USLE without considering the C (cover) and P (practice) factors.

Avoided export – This metric quantifies vegetation's role in reducing erosion at the pixel level and trapped sediment transported from upslope areas, preventing it from reaching a river downstream. Essentially, it represents the total retained sediment on a pixel. Avoided export is a key indicator of the ecosystem service value from the perception of downriver water users and is computed as follows:

$$AEXi = (RKLSi - USLEi) \cdot SDRi + Ti \quad (16)$$

AEXi represents the total sediment retention on a pixel, accounting for both on-pixel erosion control and sediment trapped from upslope sources. By capturing this sediment, the landscape helps reduce

the total sediment exported to streams. Similar to avoided erosion, the difference between RKLSi and USLEi highlights the role of vegetation and effective land management actions in preventing erosion. By multiplying this difference by the SDRi, the model quantifies the portion of erosion initiated from that pixel that does not reach a stream. Finally, Ti represents the sediment from upslope areas retained on pixel i, preventing further transport into a stream.

RESULT AND DISCUSSION

The elevation map of the Haraz River Basin (Fig. 3) indicates that the lowest elevation in the region is 213 meters, located at the basin's outlet. In comparison, the highest elevation is 5,595 meters, corresponding to Mount Damavand. Consequently, the elevation difference within the basin exceeds 5,000 meters.

Fig. 4 represents the rainfall erosivity factor (R) in the watershed, a key component of the RUSLE.

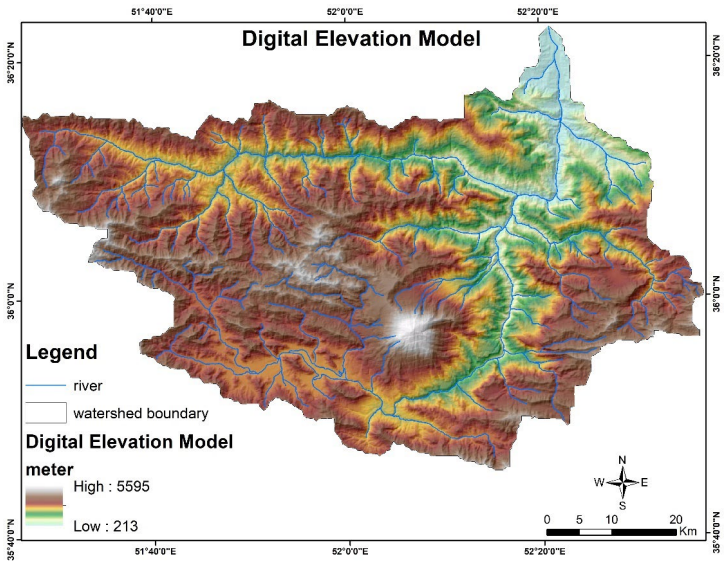

Fig. 3: DEM of the study area

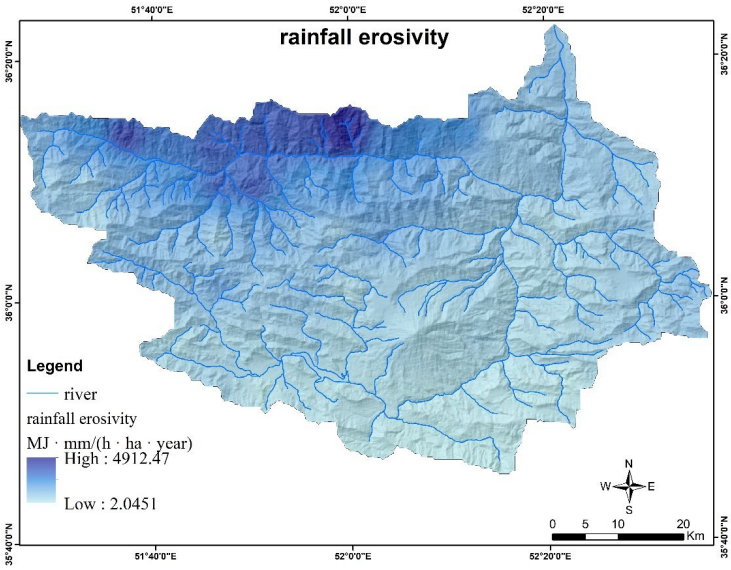

Fig. 4: Rainfall erosivity in the study area

Rainfall erosivity measures precipitation's potential to cause soil erosion and is expressed in units of MJ·mm/(h·ha·year). The values of this factor range from 2.0451 (indicating the lowest erosivity, shown in light blue) to 4912.47 (indicating the highest erosivity, shown in dark blue). Areas with high precipitation erosivity, shown in dark blue, are mainly located in the northern sections of the catchment area. Intense, energy-rich rainfall makes these areas more susceptible to significant soil erosion. In contrast, regions with low rainfall erosivity are mainly located in the central and southern parts of the watershed (shown in light blue), where rainfall is less intense and less erosive.

Fig. 5 illustrates the soil erodibility factor (K), which quantifies soil susceptibility to erosion under standardized conditions. The values of this factor range from 0.0206 (for low erodibility, represented by lighter colors) to 0.0378 (for high erodibility, represented by darker colors) and are measured in t-h-ha/(ha-MJ-mm). Soil erodibility depends on soil texture, organic matter content, permeability, and structure. The darker areas on the map, concentrated in certain regions, represent soils with higher erodibility, i.e., they are more susceptible to erosion when exposed to rainfall or surface runoff. These areas are likely to have sandy or silty textures, low organic matter content, and poor structure, making them less resistant to detachment and transport by water. In contrast, the lighter areas indicate soils with lower erodibility, potentially more stable and less prone to erosion due to higher clay content, improved soil structure, or greater organic matter content.

Fig. 6 represents the distribution of land use and land cover in the study area, calculated and analyzed based on the dataset and the total area (404,500 hectares). The results show that pastureland, which occupies 89.93% of the total area (equivalent to 363,675.6 hectares), is the predominant land use type and is vital for maintaining the ecological balance in the region. Forests, which account for 6.54% (26,459.64 hectares), are mainly located in the northeastern parts of the area and contribute significantly to the protection of soil and water resources. In contrast, barren lands and built-up areas constitute 2.37% (9,588.24 hectares) and 1.28% (5,181.12 hectares) of the total area, respectively, representing regions susceptible to erosion and urban development. Agricultural lands cover only 0.24% (990.72 hectares), indicating limited agrarian activities in the region. Surface water, which accounts for 0.11% (427.68 hectares), is mainly distributed along the river network and reflects the spatial distribution of water resources. Snowpack accounts for the smallest share

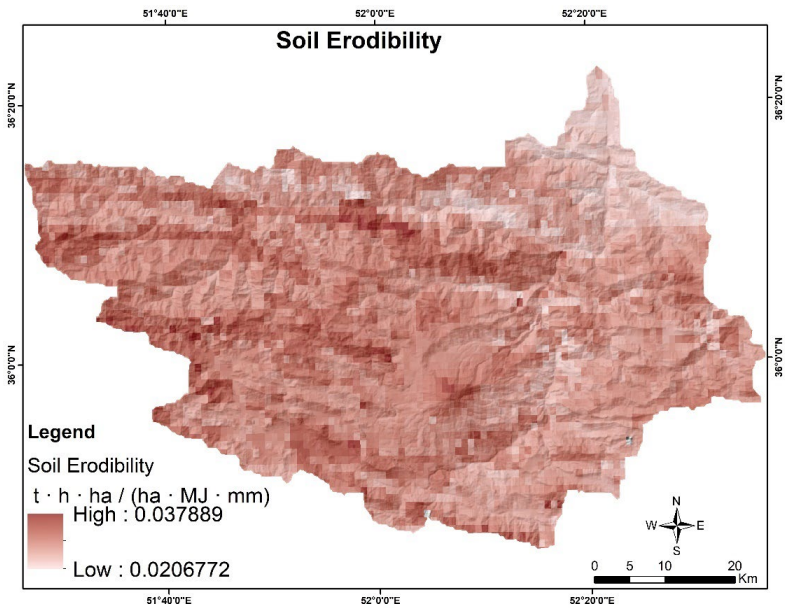

Fig. 5: Soil erodibility in the study area

at 0.03% (110.16 hectares) and is observed at higher elevations. This analysis revealed that grasslands and forests are important components of the regional ecosystem. At the same time, wastelands and croplands require special management to mitigate erosion risks and ensure ecological sustainability. The spatial distribution provides valuable information for managing the region's natural resources, preserving soil and water, and sustainable planning.

Lucode 1:

USLE_C = 0: Represents water bodies. USLE_P = 0.1: Indicates strong erosion control measures have been implemented, significantly reducing the risk of erosion.

Lucode 2:

USLE_C = 0.01: This type of land cover (e.g., forests or protected vegetation) has the highest capacity to prevent soil erosion. USLE_P = 0.8: Some management practices are applied but are less effective compared to Lucode 1.

Lucode 3:

USLE_C = 0.25: Indicates moderate susceptibility to erosion, likely associated with agricultural lands or disturbed areas. USLE_P = 0.85: Basic erosion control measures are in place with moderate effectiveness.

Lucode 4:

USLE_C = 0.05: Represents low susceptibility to erosion, possibly indicative of areas with partial vegetation cover or artificial lands. USLE_P = 1: No erosion control measures have been implemented.

Lucode 5:

USLE_C = 0.7: High susceptibility to erosion, likely representing barren or poorly managed agricultural lands. USLE_P = 1: No erosion control measures are implemented, increasing erosion risk.

Lucode 6:

USLE_C = 0: Indicates no contribution to soil erosion, likely representing snow-covered areas or permanent covers. USLE_P = 1: No need for erosion control measures.

Lucode 7:

USLE_C = 0.02: Very low susceptibility to erosion, possibly representing managed rangelands or semi-

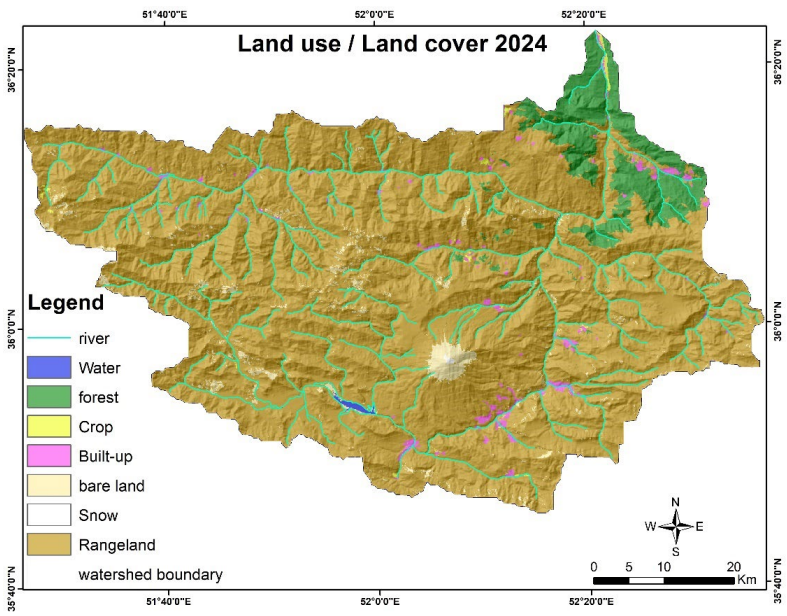

Fig. 6: Land Use and Land Cover (LU/LC) Map of the Haraz River Basin. This figure displays the spatial distribution of major land cover types, including pasturelands, forests, and barren areas. Understanding LU/LC distribution is essential for identifying erosion-prone zones and evaluating their contribution to sediment export and retention within the watershed.

natural lands. USLE_P = 0.9: Basic erosion control measures are present but are not highly effective (Table 1).

The flow accumulation threshold in this study was determined using a flow direction map extracted from the DEM. The Threshold was calculated using the formula Threshold = 0.01 to 0.05 × Maximum Flow Accumulation, resulting in a flow accumulation threshold of 300. The Borselli K parameter is a dimensionless factor used in Eq. 8 of the SDR model. This parameter is critical for determining sediment transport efficiency within the watershed and determines the sediment movement from the hillslopes into the stream network. The default value of this parameter is 2, but it can be changed depending on the specific characteristics of the watershed or calibration requirements. Accurate determination of the Borselli K parameter improves the model's performance and ensures realistic sediment delivery predictions. The Borselli IC0 parameter is another dimensionless factor used in Eq. 8 of the SDR model. It plays a significant role in modeling the relationship between the efficiency of sediment transport and the distance the sediment travels. The default value for this parameter is 0.5, but it can be changed depending on the particular characteristics of the watershed or calibration requirements. Careful determination of this parameter is crucial for improving model accuracy

Table 1: Biophysical properties of that LULC class

lucode	usle_c	usle_p
1	0	0.1
2	0.01	0.8
3	0.25	0.85
4	0.05	1
5	0.7	1
6	0	1
7	0.02	0.9

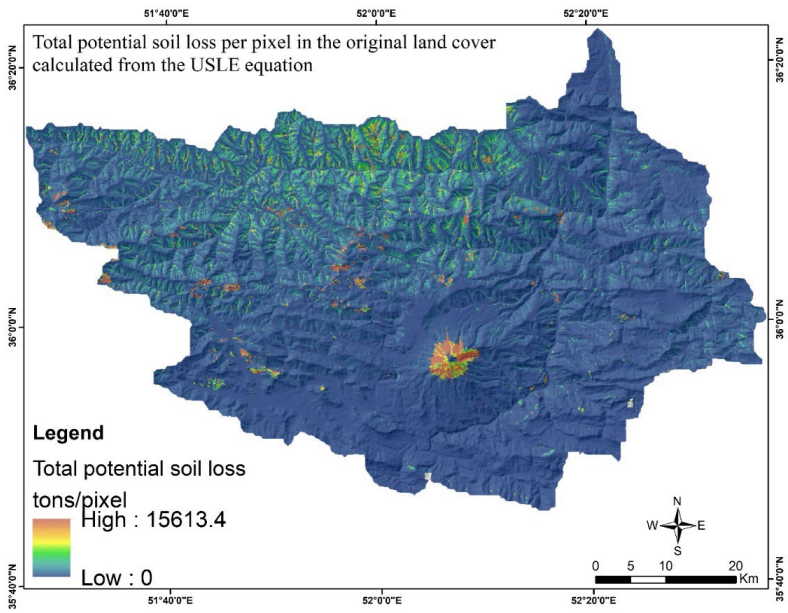

Fig. 7: Total potential soil loss in the study area (based on the USLE equation)

and more realistic sediment transport predictions. The maximum SDR value (required, dimensionless) represents the upper limit of the SDR that a pixel can have. This value is used in Eq. 8 and depends on soil texture. Specifically, it is demarcated as the portion of surface soil particles smaller than coarse sand (1,000 microns) (Vigiak *et al.*, 2012). This parameter can be calibrated in advanced studies. The default value is 0.8, but it can be adjusted depending on the soil characteristics of the study area. Proper selection of this parameter is critical for improving model precision and sediment transport predictions. The maximum L value (required, dimensionless) represents the maximum permissible value for the LS factor's slope length parameter (L). All L values that exceed this limit are limited to the specified maximum. The default value for this parameter is 122, but reasonable values given in the scientific literature range from 122 to 333 (Desmet and Govers, 1996; Renard *et al.*, 1997). Appropriate adjustment of this parameter is crucial for accurately calculating the LS factor and its impact on soil erosion predictions. It can be modified based on the topographic characteristics of the study area. In this study, a maximum L value of 200 was used. Fig. 7 illustrates the total soil erosion potential for each pixel in the primary land cover, calculated using the USLE equation. This potential incorporates the C and P factors and represents soil erosion for land under specific land use/ cover conditions. As observed, the erosion potential in this scenario ranges from 0 to 15,613 tons per hectare.

Fig. 8 illustrates the total exported sediment from any pixel and delivered to the stream network. The sediment export ranges from 0 to 3,871 tons per hectare. This map shows the total sediment exported per pixel (in tons/pixel) across the watershed. Sediment export values range from 0 tons/pixel (low sediment export, shown in blue) to 3,871 tons/pixel (high sediment export, shown in red). Areas with the maximum sediment export are condensed as local hotspots, especially on steep slopes or in regions with sparse vegetation. Red and orange critical areas indicate zones where erosion contributes significantly to sediment input into the rivers. In contrast, a remarkable area of the watershed, shown in blue and green, has low sediment export due to well-constructed soil conditions and effective sediment retention. This map depicts the spatial variability of sediment export and emphasizes the importance of implementing erosion control actions in high-risk areas to reduce sediment production and its downstream impacts.

Fig. 9 below depicts the total exported sediment for any sub-watershed. This map illustrates the

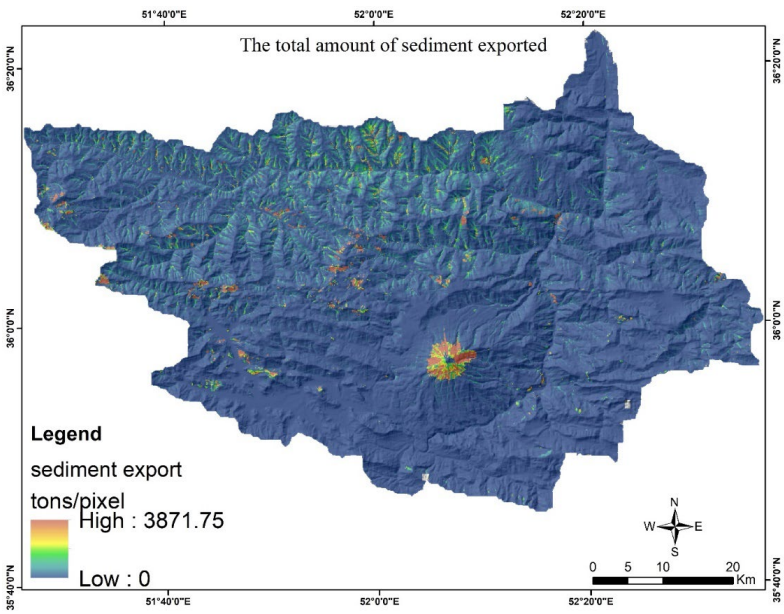

Fig. 8: Total sediment export in the study area

amount of sediment delivered to streams from each sub-watershed in the basin, measured in tons per sub-watershed. Sub-watershed 2, with a total sediment export of 1,992,277 tons, displayed in dark red, has the highest sediment export. This is likely due to steep slopes or intensive land use in this area. In contrast, sub-watershed 5, with a total sediment export of 9,328 tons, shown in blue, has the lowest sediment export, indicating effective soil management or favorable land and vegetation conditions. Other sub-watersheds exhibit varying sediment export levels, with moderate values observed in sub-watersheds 1, 4, and 7 (depicted in green and yellow) and higher values in sub-watersheds 6, 8, and 9 (depicted in orange). Overall, this spatial distribution identifies critical areas requiring management interventions to reduce erosion, particularly in sub-watershed 2, while highlighting the sustainability of practices in sub-watershed 5.

Fig. 10 illustrates the sediment delivery rate across nine sub-watersheds, ranging from 3.27 tons/hectare to 42.79 tons/hectare. Sub-watershed three, marked in red, exhibits the highest sediment delivery rate (42.79 tons/hectare), indicating severe soil erosion. Steep slopes, sparse vegetation, or intensive land-use activities likely cause this condition. Other sub-watersheds with high sediment delivery rates include sub-watersheds 6, 7, and 9, highlighted in orange. These areas may face similar erosion challenges and require soil conservation actions. Sub-watersheds 1 and 4, represented in blue, show the lowest sediment delivery rates (3.27–3.64 tons/hectare). These areas likely feature low slopes, better vegetation cover, or more effective soil management practices. These sub-watersheds can serve as models for implementing conservation strategies in high-risk areas. Sub-watersheds 8 and 5 have moderate sediment delivery rates (3.88–7.99 tons/hectare), indicating balanced conditions where moderate erosion risks coexist with some natural or human-induced controls. The northern sub-watersheds, such as sub-watershed 3, and the southern sub-watersheds, including 6, 7, and 9, are more vulnerable to erosion. In contrast, central and eastern sub-watersheds, such as 1, 4, and 5, demonstrate lower sediment delivery rates. This analysis highlights critical areas requiring erosion control measures and provides insights into leveraging the conditions in low-erosion sub-watersheds to mitigate risks in high-erosion zones.

Sub-watershed 2:

The highest USLE_Tot value (13,016,268 tons) indicates that this sub-watershed has the greatest potential for soil erosion. The high value of Sed_

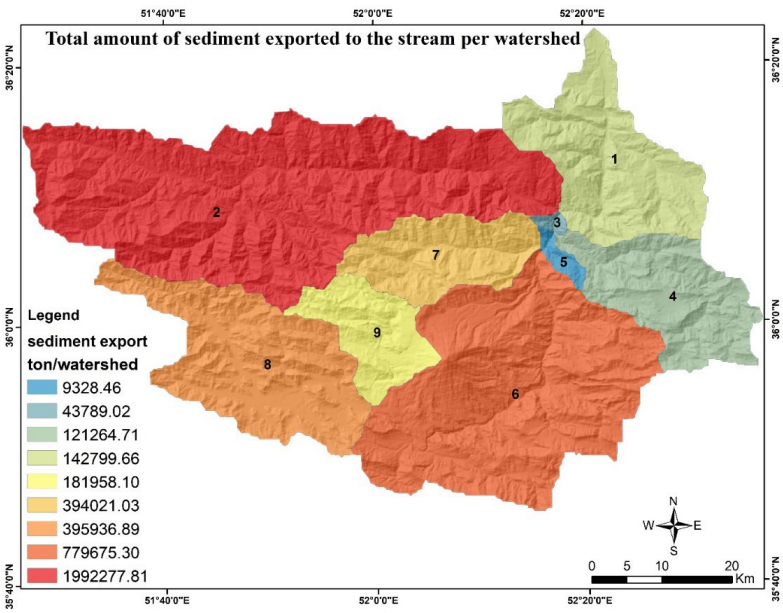

Fig. 9: Total sediment export of each sub-watershed

Export (1,992,277 tonnes) mirrors a huge sediment transport into the rivers, while a substantial part of the sediment (7,467,088 tonnes) is deposited within the sub-basin. The high values of Avoid_Exp and Avoid_Eros showed that vegetation cover is crucial for reducing sediment export and soil conservation (Table 2).

Subwatershed 5:

The lowest USLE_Tot value (60,721 tonnes) and Sed_Export value (9,328 tonnes) reflect minimal erosion and sediment transport. Because of its natural or managed characteristics, this subwatershed generates and exports significantly less sediment, indicating its stability.

Sub-watershed 7:

A relatively high Sed_Export value (394,021 tons) and significant deposited sediment (1,784,968 tons) show that this sub-watershed plays an important role in sediment transport to streams. However, it also retains a considerable portion of sediment within its boundaries. This analysis provides a comprehensive understanding of sediment dynamics and the role

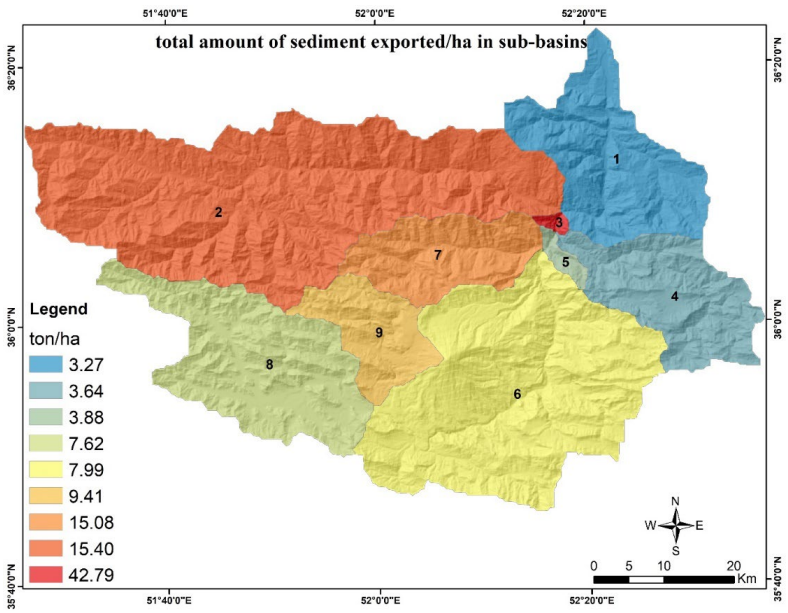

Fig. 10: Sediment Export of each sub-watershed (ton/ha)

Table 2: Erosion and sediment in each sib-watershed

ws_id	usle_tot	sed_export	sed_dep	avoid_exp	avoid_eros
1	1065043.58	142799.66	674584.72	8795877.75	75351901
2	13016268.06	1992277.87	7467088.04	62749964.5	517662540
3	178137.16	43789.02	87910.14	470086.66	2211622.25
4	830865.47	121264.7	473293.12	5415447.13	40070433.5
5	60721.23	9328.46	47877.05	523386.1	3129602.5
6	3444148.2	779675.3	2467061.01	9793981.85	49756400.88
7	2198022.09	394021.04	1784968.44	11303677.5	62681980
8	2210906.43	395936.89	1369691.46	6644613.52	49522931.06
9	1049863	181958	922308	2920707	14631887

of management practices in reducing soil erosion. Sub-watersheds with high USLE_Tot and Sed_Export values (e.g., Sub-watershed 2) require more intensive management interventions to control erosion and reduce sediment transport. In contrast, sub-watersheds with lower values (e.g., Sub-watershed 5) exhibit greater stability and can serve as reference areas for planning sustainable management strategies.

Sedexport (units: tons per watershed): Represents the total exported sediment to the stream within a watershed. This value should be compared with the observed sediment loading at the watershed outlet. Understanding the hydrologic regime of the watershed and the involvement of overland/ sheetwash sediment in total sediment yield aids in adjusting and calibrating the model. (Derived from Eq. 10, with the sum calculated over the watershed area).

Usletot (units: tons per watershed): Denotes the total potential soil loss within any watershed, estimated using the USLE formula. (Calculated as the sum of USLE values from (1) over the watershed area).

Avoidexp (units: tons per watershed): Represents the total avoided sediment export in the watershed, calculated as the sum of AEXi values from (16) over the entire watershed area.

Avoideros (units: tons per watershed): Refers to the total avoided of local erosion avoided within the watershed, obtained by summing AERi values from (15) across the watershed.

Seddep (units: tons per watershed): Indicates the total sediment deposited within the watershed that does not reach the stream. This is determined by summing Ti values from (13) across the watershed area.

Our findings on sediment retention variability align partially with Borrelli *et al.,* (2017), who noted that land cover, especially vegetation, significantly reduces soil erosion at the global scale. However, unlike Borrelli's global models, our study incorporates high-resolution local inputs and topographic heterogeneity, revealing more granular spatial differences across sub-watersheds, particularly between sub-watersheds 2 and 5. This contrast underscores the value of detailed ecosystem service-based assessments at the local level. The identified sediment retention hotspots not only play a critical role in reducing sediment delivery to streams but also contribute significantly to various ecosystem services. By trapping sediments before they reach water bodies, vegetated areas help decrease turbidity and limit the transport of sediment-bound pollutants, thereby enhancing water purification and improving downstream water quality. Moreover, sediment control structures and natural vegetation increase soil infiltration and reduce surface runoff, which supports flood regulation and helps attenuate peak flows. Additionally, by preserving topsoil and retaining essential nutrients, these areas help maintain soil fertility, contributing to long-term agricultural productivity and the ecological resilience of the watershed.

CONCLUSION

The results revealed that areas with sharp slopes and sparse vegetation, such as sub-watershed 2, are most at risk of erosion and sediment transport. Contrary to this, sub-watersheds with dense vegetation, such as sub-watershed 5, effectively prevented erosion and sediment transport. These results align with previous studies, such as those by Vigiak *et al*., (2012) and Borrelli *et al*., (2017), which introduced vegetation cover and topography as key factors in reducing erosion and sedimentation. Compared to these studies, this study used high-resolution local data, providing a more detailed spatial distribution pattern of erosion and sediment transport. One of this study's strong points is using advanced tools, such as the SDR model, in combination with local data, which allows a more detailed analysis of erosion and sediment dynamics. Compared to similar studies, such as Renard *et al*., (1997), this study provides a more detailed analysis of local factors, including land use and the spatial distribution of vegetation cover. For example, including land use maps from 2024 and high-resolution DEM data led to more accurate results than generalized models. Furthermore, the results showed that vegetation cover and management practices significantly influence erosion and sediment control. For example, the high values of avoided erosion and export in areas with enhanced protection measures emphasize the effectiveness of these practices. These results are consistent with the work of Desmet & Govers (1996), who stressed that proper land management can significantly reduce erosion. Overall, the results of this study emphasize the

complex interplay between natural and management factors in controlling erosion and sediment transport. Overconfirming previous research findings, this study adds value by providing detailed spatial maps and an in-depth analysis of sediment-related ecosystem services. Concisely, management strategies that focus on improving vegetation cover, changing land use, and installing sediment barriers could improve watershed management in the Haraz Basin and serve as a model for similar watersheds. The findings of this study demonstrate the critical influence of topography, vegetation cover, and land management on sediment retention and erosion dynamics across the Haraz River Basin. Areas such as sub-watershed 2, which exhibited the highest erosion and sediment export rates, indicate an urgent need for targeted afforestation, slope stabilization, and erosion control interventions. In contrast, the stability observed in sub-watershed 5 highlights the benefits of effective land management and vegetation cover in mitigating soil loss. These results underscore the potential of integrating ecosystem service assessments with sediment modeling tools like InVEST to inform spatially explicit conservation planning. For future research, incorporating seasonal variability in precipitation and sediment transport could further refine our understanding of erosion processes and support the development of more adaptive, climate-responsive watershed management strategies.

AUTHOR CONTRIBUTIONS

A. Chahkandi performed the Conceptualization, Literature Review, Data Collection, Methodology, Software, and Manuscript Preparation (Writing – original draft). G.R. Nabi Bidhendi and B. Malekmohammadi performed supervision, validation, project administration, and review and edit of the manuscript.

ACKNOWLEDGEMENT

This study is part of the first author's doctoral thesis at the University of Tehran. The authors would like to express their sincere gratitude to the University of Tehran for its valuable support and collaboration in facilitating the successful completion of this research

CONFLICT OF INTEREST

The authors declare no conflict of interest regarding the publication of this work. In addition, they have witnessed ethical issues, including plagiarism, informed consent, misconduct, data fabrication, falsification, double publication or submission, and redundancy.

ABBREVIATIONS (NOMENCLATURE)

DEM	Digital Elevation Model
GIS	Geographic Information System
IC	Connectivity Index
InVEST	Integrated Valuation of Ecosystem Services and Tradeoffs
IRIMO	Iran Meteorological Organization
LU/LC	Land Use /Land Cover
MFD	Multiple-Flow Direction
RUSLE	Revised Universal Soil Loss Equation
SRTM	Shuttle Radar Topography Mission
SDR	Sediment Delivery Rate

REFERENCES

Andualem, T. G.; Hewa, G. A.; Myers, B. R.; Boland, J.; Peters, S., (2024). Predicting Suspended Sediment Transport in Urbanised Streams: A Case Study of Dry Creek, South Australia. Hydrology., 11(11): 1-16 (**16 pages**).

Balist, J.; Malek Mohammadi, B.; Jafari, H. R.; Nohegar, A., (2021). Water Resources Supply and Demand Modeling using the Concept of Ecosystem Services in Sirvan Transboundary Basin. Environ and Water Eng., 7(2): 279-292 **(14 pages)**. (In Persian)

Balist, J.; Malekmohammadi, B.; Jafari, H.R.; Geneletti, D., (2022). Detecting land use and climate impacts on water yield ecosystem service in arid and semi-arid areas. A study in Sirvan River Basin-Iran. Appl Water Sci., 12(4): 1-14 **(14pages).**

Balist, J.; Malekmohammadi, B.; Jafari, H.R.; Geneletti, D., (2022). Modeling the supply, demand, and stress of water resources using ecosystem services concept in Sirvan River Basin (Kurdistan-Iran). Water Sply., 22 (3): 2816–2831 **(15 pages).**

Bhattarai, R.; Dutta, D.; (2006). Estimation of Soil Erosion and Sediment Yield Using GIS at Catchment Scale. Water Resour. Manag., 21: 1635–1647 **(12 pages)**.

Borrelli, P.; Robinson, D. A.; Panagos, P.; Lugato, E.; Yang, J. E.; Alewell, C.; Ballabio, C., (2017). Land use and climate change impacts on global soil erosion by water (2015-2070). Proce. Nat. Acad. Scences., 114(36): 9313-9318 **(6 pages)**.

Borselli, L.; Cassi, P.; Torri, D., (2008). Prolegomena to sediment and flow connectivity in the landscape: A GIS and field numerical assessment. Catena., 75: 268–277 **(9 pages)**.

Cavalli, M.; Trevisani, S.; Comiti, F.;, Marchi, L., (2013). Geomorphometric assessment of spatial sediment connectivity in small Alpine catchments. Geomorphology., 188: 31–41 **(10 pages)**.

Costanza, R.; de Groot, R.; Braat, L.; Kubiszewski, I.; Fioramonti, L.; Sutton, P.; Grasso, M., (2017). Twenty years of ecosystem services: How far have we come and how far do we still need to go. Ecos. Serv., 28: 1-16 **(16 pages).**

Desmet, P.J.J.; Govers, G.; (1996). A GIs procedure for automatically calculating the USLE LS factor on topographically complex landscape units. J. Soi., 51(5): 427–433 **(7 pages).**

Dominati, E.; Patterson, M.; Mackay, A., (2010). A framework for classifying and quantifying the natural capital and ecosystem services of soils. Ecol. Econ., 69(9): 1858-1868 **(10 pages).**

Fang, H.; He, G.; Huang, L.; Zhao, Ch.; Wang, J.; Han, Y.; Gao, Q.; Zhang, T.; Meng, J., (2024). Altered flow and sediment transport impacts on the ecosystems of Chinese major rivers: An urgent call for ecofluvial dynamics. River., 3: 341–361 **(20 pages).**

Fu, B.; Wang, Y. K.; Lu, Y. H.; & Liu, S. L., (2011). The effects of land-use combinations on soil erosion: A study in the Loess Plateau of China. Jour. Hydro., 410(3-4): 230-239 **(19 pages).**

Guo, Q; Jin, YeeChung., (2002). Modeling Nonuniform Suspended Sediment Transport in Alluvial Rivers., Jour.Hydr. Eng., 9: 839-847 **(8 pages).**

Hamel, P.; Chaplin-Kramer, R.; Sim, S.; Mueller, C., (2015). A new approach to modeling the sediment retention service (InVEST 3.0): Case study of the Cape Fear catchment, North Carolina, USA. Sci. Tot. Enviro., 524–525: 166–177 **(11 pages)**.

Hamel, P; Bryant, B., (2017). Uncertainty assessment in ecosystem services analyses: Seven challenges and practical responses. Ecos. Serv., 24: 1-15 **(15 pages).**

Lopez-vicente, M.; Poesen, J.; Navas, A.; Gaspar, L., (2013). Predicting runoff and sediment connectivity and soil erosion by water for different land use scenarios in the Spanish Pre-Pyrenees. Catena., 102: 62–73 **(11 pages)**.

Malekmohammadi B.; Rezaei M.; Balist J.; Yaghoobi. A. A., (2023). Effects of floods on the oil, gas, and petrochemical industries: case study in Iran. Cris. Oil, Gas. Petro. Ind., 103-133 **(30 pages).**

Oliveira, A.H.; Silva, M.A. da.; Silva, M.L.N.; Curi, N.; Neto, G.K.; Freitas, D.A.F. de., (2013). Development of Topographic Factor Modeling for Application in Soil Erosion Models., Soil Pro. Curr. Tre. Qual. Asses., 1: 1-28 **(28 pages).**

Owens, Philip N., (2020). Soil erosion and sediment dynamics in the Anthropocene: a review of human impacts during a period of rapid global environmental change. J. Soi. Sedi., 20: 4115–4143 **(27 pages).**

Pimentel, D.; Harvey, C.; Resosudarmo, P.; Sinclair, K.; Kurz, D.; McNair, M.; Blair, R., (1995). Environmental and economic costs of soil erosion and conservation benefits. Science., 267(5201): 1117-1123 **(6 pages).**

Posthumus, H.; Rouquette, J. R.; Morris, J.; Gowing, D. J.; Hess, T. M., (2010). A framework for the assessment of ecosystem goods and services; a case study on lowland floodplains in England. Ecol. Econ., 69(6): 1510-1523 **(13 pages).**

Renard, K.; Foster, G.; Weesies, G.; McCool, D.; Yoder, D., (1997). Predicting Soil Erosion by Water: A Guide to Conservation Planning with the Revised Universal Soil Loss Equation (RUSLE). U.S. Dep. Agri., Washington DC.

Renard, K.; Freimund, J., (1994). Using monthly precipitation data to estimate the R-factor in the revised USLE. J. Hydrol., 157: 287–306 **(19 pages).**

Rodriguez, B.C.; Palma-Torres, V. M.; Castaeda, TJ.E.; Codtiyeng, S.K.; Castillo, J.F.; Sasi, A.P.V.; Tercero, M.U.; Andrada, R.T.; and Andrada, R.T., (2023). Drivers and Impacts of Land Use and Land Cover Changes on Ecosystem Services Provided by the Watersheds in the Philippines: A Systematic Literature Review. Int.l for. rev., 25(4): 473-490 **(18 pages).**

Roose., (1996). Land husbandry - Components and strategy. Soi. Bull., 70. Rome.

Sadeghi, A.; Galalizadeh, S.; Zehtabian, G.; Khosravi, H.; (2021). Assessing the change of groundwater quality compared with land-use change and precipitation rate (Zrebar Lake's Basin). Appl Water Sci., 11: 1-15 **(15 pages).**

Sadeghi, A.; Khaledi, J.; Nyman, P., (2018). Rainfall Variability and Land-Use Change in Arid Basins with Traditional Agricultural Practices; Insight from Ground Water Monitoring in Northwestern Iran. J Earth Sci Clim Change., 9 (11): 491-498 **(7 pages).**

Sadeghi, A.; Zehtabian, G.; Malekian, A.; Khosravi, H., (2014). The Effect of Land use Changes on Groundwater Quality (Case Study: Zaribar Lake Basin). Wat. Man. Res., 27(4): 90-97 **(7 pages).**

Schröter, M.; Zanden, E. H.; van Oudenhoven, A. P. E.; Remme, R. P.; Serna-Chavez, H. M.; de Groot, R. S.; Opdam, P., (2014). Ecosystem services as a contested concept: A synthesis of critique and counter-arguments. Cons. Let., 7(6), 514-523 **(9 pages).**

Slosson, J.; Kelleher, C.; Hoke, G., (2021). Contrasting Impacts of a Hotter and Drier Future on Streamflow and Catchment Scale Sediment Flux in the High Andes. Journal of Geophysical Research: Eart. Sur., 126 (8): 1-20 **(20 pages).**

Sougnez, N.; Wesemael, B. Van.; Vanacker, V., (2011). Low erosion rates measured for steep, sparsely vegetated catchments in

southeast Spain. Catena., 84: 1–11 **(10 pages).**

Tabarestani, E Sh.; Afzalimehr, H.; and Sui, J., (2022). Assessment of Annual Erosion and Sediment Yield Using Empirical Methods and Validating with Field Measurements Case Study. Wat., 14 (10): 1-16 **(16 pages).**

Tedesco, P.; Beier, C. M.; & Johnson, S. L., (2020). Modeling sediment delivery in response to land use and climate change using the InVEST tool: Case studies from New York and Oregon, USA. Enviro. Mod. & Soft., 132: 1-20 **(20 pages).**

Vigiak, O.; Borselli, L.; Newham, L.T.H.; Mcinnes, J.; Roberts, A.M., (2012). Comparison of conceptual landscape metrics to define hillslope-scale sediment delivery ratio. Geomor., 138: 74–88 **(14 pages).**

Zebardast, L.; Balist, J.; Karimi, H., (2023). Integrated Environmental Assessment of Unsustainable Exploitation and Pollution of Shared Water Resources in Transboundary Basins of Semi-arid and Arid Regions. Case Study: Tigris-Euphrates River Basin. Poll., 9(4): 1475-1495 **(20 pages).**

HOW TO CITE THIS ARTICLE

Chahkandi, A.; Nabi Bidhendi, G. R.; Malekmohammadi, B., (2026). Modeling sediment transport and assessing erosion and sedimentation status in the Haraz River watershed based on the ecosystem services concept. Int. J. Hum. Capital. Urban Manage., 11(1): 33-50.

DOI: 10.22034/IJHCUM.2026.01.03

URL: https://www.ijhcum.net/article_724954.html